

University of Wollongong

Research Online

Faculty of Science, Medicine and Health -
Papers: part A

Faculty of Science, Medicine and Health

1-1-2014

Photodissociation of TEMPO-modified peptides: new approaches to radical-directed dissociation of biomolecules

David L. Marshall
University of Wollongong, d1m418@uowmail.edu.au

Christopher S. Hansen
University of Wollongong, csh297@uowmail.edu.au

Adam J. Trevitt
University of Wollongong, adamt@uow.edu.au

Han Bin Oh
Sogang University

Stephen J. Blanksby
University of Wollongong, blanksby@uow.edu.au

Follow this and additional works at: <https://ro.uow.edu.au/smhpapers>

 Part of the [Medicine and Health Sciences Commons](#), and the [Social and Behavioral Sciences Commons](#)

Recommended Citation

Marshall, David L.; Hansen, Christopher S.; Trevitt, Adam J.; Oh, Han Bin; and Blanksby, Stephen J., "Photodissociation of TEMPO-modified peptides: new approaches to radical-directed dissociation of biomolecules" (2014). *Faculty of Science, Medicine and Health - Papers: part A*. 1459.
<https://ro.uow.edu.au/smhpapers/1459>

Research Online is the open access institutional repository for the University of Wollongong. For further information contact the UOW Library: research-pubs@uow.edu.au

Photodissociation of TEMPO-modified peptides: new approaches to radical-directed dissociation of biomolecules

Abstract

Radical-directed dissociation of gas phase ions is emerging as a powerful and complementary alternative to traditional tandem mass spectrometric techniques for biomolecular structural analysis. Previous studies have identified that coupling of 2-[(2,2,6,6-tetramethylpiperidin-1-oxyl)methyl]benzoic acid (TEMPO-Bz) to the N-terminus of a peptide introduces a labile oxygen-carbon bond that can be selectively activated upon collisional activation to produce a radical ion. Here we demonstrate that structurally-defined peptide radical ions can also be generated upon UV laser photodissociation of the same TEMPO-Bz derivatives in a linear ion-trap mass spectrometer. When subjected to further mass spectrometric analyses, the radical ions formed by a single laser pulse undergo identical dissociations as those formed by collisional activation of the same precursor ion, and can thus be used to derive molecular structure. Mapping the initial radical formation process as a function of photon energy by photodissociation action spectroscopy reveals that photoproduct formation is selective but occurs only in modest yield across the wavelength range (300–220 nm), with the photoproduct yield maximised between 235 and 225 nm. Based on the analysis of a set of model compounds, structural modifications to the TEMPO-Bz derivative are suggested to optimise radical photoproduct yield. Future development of such probes offers the advantage of increased sensitivity and selectivity for radical-directed dissociation.

Keywords

GeoQuest

Disciplines

Medicine and Health Sciences | Social and Behavioral Sciences

Publication Details

Marshall, D. L., Hansen, C. S., Trevitt, A. J., Oh, H. Bin. & Blanksby, S. J. (2014). Photodissociation of TEMPO-modified peptides: new approaches to radical-directed dissociation of biomolecules. *Physical Chemistry Chemical Physics*, 16 (10), 4871-4879.

**Photodissociation of TEMPO-modified peptides: New approaches to
radical-directed dissociation of biomolecules**

David L. Marshall¹, Christopher S. Hansen¹, Adam J. Trevitt¹, Han Bin Oh²,

Stephen J. Blanksby^{1*}

¹ARC Centre of Excellence for Free Radical Chemistry and Biotechnology, School of
Chemistry, University of Wollongong, NSW, 2522, AUSTRALIA

²Department of Chemistry, Sogang University, Seoul 121-742, KOREA

*** Corresponding author**

Prof. Stephen J. Blanksby

School of Chemistry, University of Wollongong

Northfields Ave, Wollongong, NSW 2522

AUSTRALIA

Ph: +61 2 4221 5484

Fax: +61 2 4221 4287

Email:

blanksby@uow.edu.au

Abstract

Radical-directed dissociation of gas phase ions is emerging as a powerful and complementary alternative to traditional tandem mass spectrometric techniques for biomolecular structural analysis. Previous studies have identified that coupling of 2-[(2,2,6,6-tetramethylpiperidin-1-oxyl)methyl]benzoic acid (TEMPO-Bz) to the *N*-terminus of a peptide introduces a labile oxygen-carbon bond that can be selectively activated upon collisional activation to produce a radical ion. Here we demonstrate that structurally-defined peptide radical ions can also be generated upon UV laser photodissociation of the same TEMPO-Bz derivatives in a linear ion-trap mass spectrometer. When subjected to further mass spectrometric analyses, the radical ions formed by a single laser pulse undergo identical dissociations as those formed by collisional activation of the same precursor ion, and can thus be used to derive molecular structure. Mapping the initial radical formation process as a function of photon energy by photodissociation action spectroscopy reveals that photoproduct formation is selective but occurs only in modest yield across the wavelength range (300 – 220 nm), with the photoproduct yield maximised between 235 and 225 nm. Based on the analysis of a set of model compounds, structural modifications to the TEMPO-Bz derivative are suggested to optimise radical photoproduct yield. Future development of such probes offers the advantage of increased sensitivity and selectivity for radical-directed dissociation.

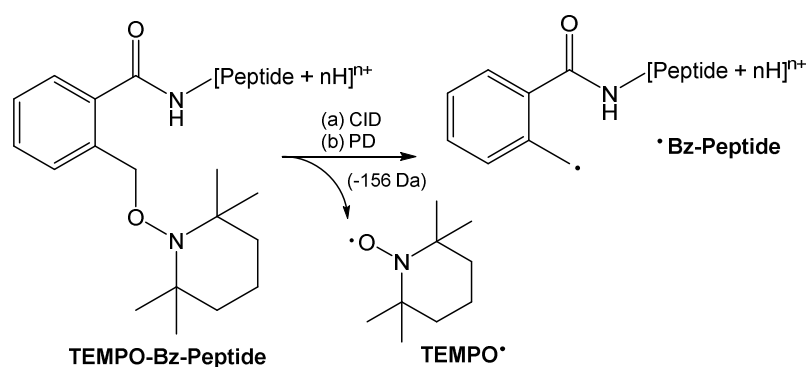
Introduction

In the field of proteomics, radical-based tandem mass spectrometry of peptides and proteins is a powerful alternative tool to collision-induced dissociation (CID). Whilst their speed and simplicity cannot be disputed, “slow-heating” methods¹ such as CID or infrared multi-photon dissociation (IRMPD) generally promote even-electron fragmentation of the peptide or protein ion, and used in isolation may not provide full sequence coverage or complete characterisation of labile post-translational modifications (PTMs).^{2, 3} Compared to CID or IRMPD, electron capture dissociation (ECD)⁴⁻⁷ and electron transfer dissociation (ETD)^{8, 9} of multiply-charged peptide/protein cations typically produce spectra with greater sequence coverage and PTM localisation, due to extensive, non-selective fragmentation.^{9, 10} Electron-induced dissociation (EID) of both protonated^{11, 12} and deprotonated¹³ singly charged peptide ions also elicits additional radical driven sequence coverage information complementary to that derived from collisional activation, without modifying the initial charge state.

The increasing importance of radical ions in biomolecular mass spectrometry has motivated development of chemical methods for introducing radical sites into peptide/protein ions that are applicable to a wider range of mass spectrometer configurations. For example, CID of ternary metal/peptide complexes generate peptide radical cations,¹⁴ which produce *a/x*- or *c/z*-type peptide backbone fragments and notable side chain losses upon subsequent activation.¹⁵⁻¹⁹ Covalent attachment of a free radical precursor to peptides is another pathway to produce peptide radical ions, by introducing a labile bond that is susceptible to homolysis. Free-radical initiated peptide sequencing (FRIPS) methods offer the particular advantage of a well-defined initial radical site, thus fragmentation can be induced at specific amino acid

residues. For example, collisional activation of *N*-nitroso- and *S*-nitroso-derivatives of tryptophan and cysteine-containing peptides produce aminyl and sulfenyl radicals through bond homolysis with loss of nitric oxide. Subsequent activation of these radical ions initiates radical-driven fragmentation along the peptide backbone and thus yields a range of diagnostic product ions.²⁰⁻²⁴

Chemical modification of the *N*-terminus of the peptide or protein is another example of derivitisation for FRIPS. For instance, upon CID, peroxy-carbamates²⁵ and azo moieties²⁶ are susceptible to homolytic dissociation forming nitrogen- and carbon-centred radicals, respectively. Collisional activation of such radical ions results in side-chain and backbone cleavage with extensive sequence coverage. Lee *et al.* introduced 2-[(2,2,6,6-tetramethylpiperidin-1-oxyl)methyl]benzoic acid (TEMPO-Bz, Scheme 1) as a free radical precursor bound to peptides through the *N*-terminus or at the ϵ -amine of lysine residues,²⁷⁻²⁹ and is the tagging group employed in the present study. Collisional activation of the precursor peptide ions initiates homolytic cleavage of the labile NO-C bond, promoted by the remarkable stability of the released nitroxyl radical. Subsequent collisional activation of the peptide radical ions yields peptide backbone fragments and side-chain losses with extensive sequence coverage. Abundant formation of *a/x*- and *c/z*-type ions suggests that radical-driven peptide backbone dissociation is the major fragmentation pathway, similar to the electron-based methods.



Scheme 1: Peptide-TEMPO-Bz structure used in this study. Activation of the derivatised peptide by either (a) collision-induced dissociation (CID, shown previously) or (b) photodissociation (PD, shown here) results in homolytic cleavage of the carbon-oxygen bond, and neutral loss of the TEMPO moiety (-156 Da) to yield a peptide radical ion.

Ultraviolet photodissociation (UVPD) has also been used extensively for peptide characterisation and sequencing.³⁰ The identity and yield of photoproduct ions depends on many aspects, including the incident photon energy, chemical modifications to the peptide,³¹ ion charge-state, laser fluence, overlap between the incident light and the ion ensemble, absorption cross-section, and the number of pulses with which the ion ensemble is irradiated.³² The complexity of laser-based structural characterisation is increased for large molecules as bond dissociation can be mediated by the redistribution of excess energy among many vibrational degrees of freedom.³³ The energy required for radical formation through bond homolysis can thus exceed the intrinsic bond dissociation energy. In order to form protein radical ions in the gas phase by UV irradiation, it is therefore necessary to induce dissociation on a time scale faster than competing processes, including intramolecular vibrational energy redistribution (IVR). IVR extends the lifetime of the activated ion population and provides opportunity for non-dissociative removal of excess energy *via* collisional cooling. One such example is electron photodetachment from polyanions.³⁴ Peptide radical anions are formed by efficient UV excitation of bound $\pi^* \leftarrow \pi$ electronic transitions within aromatic amino acids, followed by crossing to unbound electronic states, leading to electron detachment on a timescale that is competitive with IVR.

Photolysis of suitable photolabile precursors is an alternative way to efficiently produce a radical site for peptide sequencing. For example, upon irradiation with 266 nm photons, iodine atom loss from aryl iodide-modified peptide ions is observed as the major

process in the mass spectrum.³⁵⁻³⁷ Kirk *et al.* recently demonstrated the wavelength dependence of iodine atom loss from iodo-tyrosines by photodissociation (PD) action spectroscopy, highlighting the influence of charge state on the efficacy of photoproduct formation.³⁸ Compared with CID, photodissociation of aryl iodides facilitates the production of radical sites without complications due to isomerisation.^{39, 40} Strategies that utilise UV radiation and a photolabile radical precursor show promise for peptide characterisation. High photoproduct yields,⁴¹ the availability of tuneable laser sources, and avoiding the low-mass cut-off inherent in ion trap-based analysis⁴² offer an opportunity for enhanced peptide sequencing coverage over collisional and electron-based tandem mass spectrometric methods. Photodissociation can access site-specific radical ion product channels, whereas collisional activation of the same precursor ion yields less selective fragmentation, a mixture of isomers, or no radical-directed dissociation at all.^{43, 44}

In the present study, we have explored the application of UVPD to TEMPO-Bz modified peptides and assessed the suitability of this strategy for FRIPS. Here we show that absorbed UV radiation induces homolytic cleavage of the labile carbon-oxygen bond in the TEMPO-Bz derivatives. Thus generated, the peptide radical ions can be further activated by CID to fragment the peptide backbone, resulting in sequence ions and diagnostic side chain losses. In this study, the factors influencing the efficacy of photodissociation are explored and strategies to enhance the selectivity and sensitivity of this approach are discussed.

Experimental:

Materials

Methanol (HPLC grade), acetic acid (99%, AR grade), and ammonium acetate (AR grade) were obtained from Ajax Fine Chemicals (now part of Thermo Fisher Scientific, Sydney, Australia). All other materials were obtained from Sigma Aldrich (Sydney, Australia). The synthesis of TEMPO-Bz conjugated peptides from commercially available 2-methylbenzoic acid methyl ester has been reported previously.²⁷ Peptide solutions of kinetensin (IARRHPYFL), bradykinin (RPPGFSPFR), and YGGFMRF were prepared at *ca.* 10 – 20 μ M, in 1:1 methanol:water solvent mixtures, with the addition of 0.1% acetic acid or 0.1% ammonium acetate to facilitate the formation of positive and negative ions, respectively. Synthesis of model compounds 1-(benzyloxy)-2,2,6,6-tetramethylpiperidine-4-carboxylic acid (**1**); 4-(((1-(benzyloxy)-2,2,6,6-tetramethylpiperidin-4-yl)oxy)carbonyl)cyclohexanecarboxylic acid (**2**); and 4-(((1-(benzyloxy)-2,2,6,6-tetramethylpiperidin-4-yl)oxy)carbonyl)benzoic acid (**3**) was undertaken based on appropriate adaptation of literature procedures. Briefly, **1** was prepared by the addition of phenylacetaldehyde, hydrogen peroxide and copper (I) to 4-carboxy-TEMPO (**1a**). 4-hydroxy-TEMPO-Bz is prepared from 4-hydroxy-TEMPO in the same manner,⁴⁵ and is subsequently esterified with the appropriate difunctional acid in the presence of *N,N'*-dicyclohexylcarbodiimide (DCC) and 4-(dimethylamino)pyridine (DMAP). Desired $[M - H]^-$ anions of (**1-3**) are produced without additional purification by diluting aliquots of the reaction mixture to a concentration of approximately 5 μ M in methanol, and subjecting these solutions to electrospray ionisation (ESI). A summary table listing all peptides investigated in

this study and the charge states that were subjected to photodissociation is provided as Supporting Information (Table S1).

Mass Spectrometry

Photodissociation experiments were performed using a Thermo Fisher Scientific LTQ linear quadrupole ion-trap mass spectrometer (San Jose, CA, USA) modified for both fixed-frequency,⁴⁶ and tunable⁴⁷ laser photodissociation experiments. Briefly, the aforementioned peptide solutions are infused into the mass spectrometer through the ESI source with instrument parameters similar to those described previously.²⁷ The TEMPO-Bz modified peptide ions are mass-selected, isolated, and thermalised (*ca.* 307 K)⁴⁸ in the helium buffer gas (2.5 mTorr helium). The ion ensemble is then irradiated with a single pulse from either a fixed-frequency (266 nm) or tunable (300 – 220 nm) nanosecond laser system, the ion trap is scanned out and a PD mass spectrum is recorded containing signals for both photoproduct ions and the intact precursor ion population. In a photodissociation action spectroscopy experiment, the photodissociation yield is calculated as a fraction of the total ion population from this mass spectrum, the laser is then tuned to the next wavelength and the process repeated. For each action spectrum, the photoproduct yields are corrected by a power spectrum (acquired offline), and plotted as a function of photon wavelength.⁴⁷

The fixed-frequency experiments are performed using the 4th harmonic (266 nm) of a Nd:YAG laser (Continuum Minilite, Santa Clara, CA, USA), delivering a 5 ns, 4 mJ pulse on demand. Tunable photodissociation experiments employ an optical parametric oscillator (OPO) fitted with a frequency-doubling unit (versaScan and uvScan, GWU-Lasertechnik, Erfstadt, Germany) pumped by the 3rd harmonic (355 nm) of a QuantaRay INDI Nd:YAG laser (Spectra-Physics, Santa Clara, CA, USA). This provides a pulsed, nanosecond photon source, tunable across the range 2500 – 220 nm, delivering *ca.* 2 mJ per pulse in the UV. This

laser operates at 10 Hz and is carefully shuttered to ensure that only a single pulse enters the ion trap at the correct stage of each MS cycle.⁴⁷

Results

Photodissociation of derivatised peptides

Electrospray ionisation of TEMPO-Bz peptide solutions produced singly and multiply charged ions, with the relative abundance of charge states dependant on ion source parameters, solvent composition, and the number of acidic and basic amino acid residues in the peptide. CID spectra resulting from the isolation and activation of $[M + nH]^{n+}$ ions (where $n = 1, 2$) of bradykinin-TEMPO-Bz are displayed in Figure 1. Prior to activation, no product ions are observed from either precursor ion. The carbon-oxygen bond energy in the TEMPO-Bz motif is estimated⁴⁹ to be only 110 kJ mol^{-1} and thus upon CID, the bond between the nitroxyl oxygen and the benzyl carbon is preferentially cleaved to form an abundant radical ion (m/z 589 and m/z 1177 for doubly and singly charged ions, Figure 1(a) and 1(c), respectively). The resulting alkyl radical initially formed at the benzylic position remains covalently tethered to the *N*-terminus of bradykinin (*cf.* Scheme 1).²⁷ Additional product ions present in low abundance are attributed to spontaneous, radical-mediated backbone cleavage (*e.g.*, c_5^+) or amino acid side chain losses (*e.g.*, -100 Da, from arginine) from the primary radical product (*vide infra*). When the isolated precursor ions are irradiated with a single, $\lambda = 266 \text{ nm}$ laser pulse (henceforth PD₂₆₆), the doubly and singly protonated ions (Figure 1(b) and 1(d), respectively) undergo TEMPO loss through carbon-oxygen bond homolysis. Despite the perceived selectivity, the yield of desired radical ions is much lower in the PD₂₆₆ spectra (less than 4% of the precursor ion abundance), compared to the almost complete conversion achieved by CID. In the PD₂₆₆ experiment, the relative abundance of the open-shell product ion is higher from the singly protonated charge state, compared to the doubly charged species.

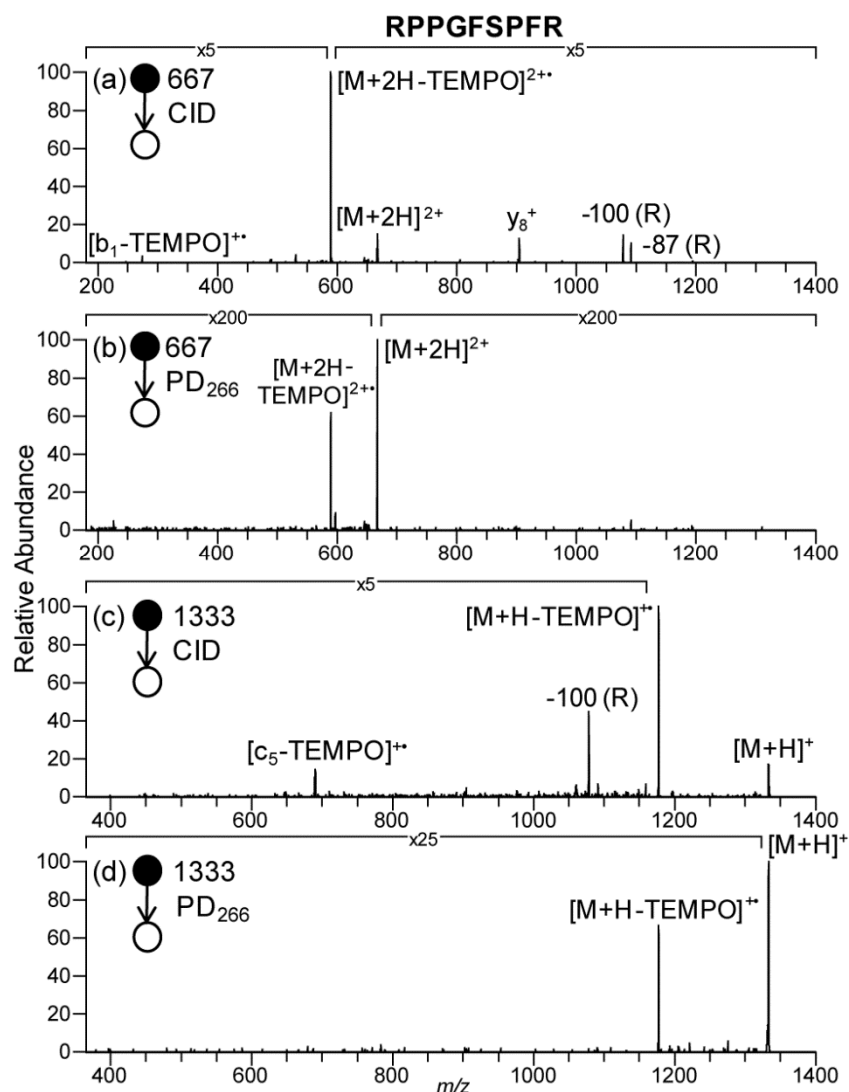


Figure 1: Mass spectra obtained upon isolation and CID (normalised collision energy of 20) or PD₂₆₆ irradiation of protonated TEMPO-modified bradykinin (RPPGFSPFR) ions, exhibiting selective loss of TEMPO; (a) CID of $[M + 2H]^{2+}$ ions; (b) PD₂₆₆ of $[M + 2H]^{2+}$ ions; (c) CID of $[M + H]^+$ ions; (d) PD₂₆₆ of $[M + H]^+$ ions. Peaks denoted by numbers represent the mass difference after TEMPO loss, and the letter in parentheses indicates the amino acid involved.

Except for the y_8^+ ion observed in the CID spectrum of derivatised bradykinin (Figure 1a), characteristic *b*-type and *y*-type product ions from the intact modified peptide, typically

observed from collisional activation of protonated peptide ions,^{50, 51} are notably minor in both the CID and PD₂₆₆ spectra. Although an intact b₁⁺ ion is not observed in Figure 1(a), a radical ion is present corresponding to formation of a b₁⁺ ion after TEMPO loss, indicating that loss of a TEMPO radical *via* homolysis is the preferred dissociation process. Additional *b*-type and *y*-type ions are present following PD₂₆₆ of the derivatised bradykinin but are of too low abundance to be readily identified at the magnifications shown in Figures 1(b) and (d). Notably however, when the abundance of *b*-type and *y*-type ions are considered relative to the abundance of the [M + xH – TEMPO]^{x+} ion (rather than the precursor ions as displayed in Figures 1b and 1d) similar peak ratios are found for PD₂₆₆ as CID spectra (see Supporting Information, Figure S1a). Indeed, some comparable *b*-type and *y*-type ions are observed in the PD₂₆₆ spectrum of unmodified bradykinin (*i.e.*, in the absence of the TEMPO-Bz tag, see Supporting Information, Figure S1b).

Activation of [M + 3H]³⁺ TEMPO-modified bradykinin ions (*m/z* 445) by CID also produces ions attributed to TEMPO loss at *m/z* 393 (see Supporting Information Figure S2). However selectivity is not retained, and the CID spectrum is dominated by ions with higher mass-to-charge ratios, indicating charge reduction fragmentation mechanisms prevail over the desired radical formation by homolysis of the oxygen-carbon bond. Likewise, irradiation of the [M + 3H]³⁺ ions by PD₂₆₆ does not result in TEMPO loss. This may be rationalised by considering that after the basic arginine residues, the final protonation site is likely to be the piperidinyll nitrogen of the TEMPO-Bz moiety. Upon protonation of the piperidinyll nitrogen, homolysis of the alkoxyamine NO-C bond is suppressed relative to even-electron rearrangement processes under CID,⁵² and we infer that analogous processes prevail upon photodissociation. Similar observations were made for other peptides when the number of charges approached or exceeded the number of basic side chains available, placing an upper limit on the charge states for which CID and PD₂₆₆ can produce the desired radical ions.⁵³

Advantageously, the TEMPO-based FRIPS methodology is also applicable to the study of negative ions.²⁹ Negative ion mass spectrometry provides structural information for proteomics that is both confirmatory and complementary to that obtained in the study of positive ions. Furthermore, for peptides with acidic residues or phosphorylation, negative ion mass spectrometry may be preferred for increased sensitivity. By contrast with positive ions, only a few studies have considered the formation and fragmentation of site-specific peptide radical anions with the aim of peptide sequencing and characterisation.^{43, 54} Singly and multiply deprotonated TEMPO-Bz peptide anions $[M - H]^-$ and $[M - 2H]^{2-}$ were produced by ESI, depending on the number of acidic residues available in the peptide. For example, isolation and PD₂₆₆ of kinetensin dianions produces the spectrum shown in Figure 2(a). It is clear from the presence of $[M - 2H]^{\bullet-}$ product ions at m/z 1442 that electron detachment competes with TEMPO photodissociation. A putative biradical anion at m/z 1286 arises from a combination of both electron detachment and bond homolysis processes. For singly charged anions (m/z 1443, Figure 2b), selective loss of TEMPO is observed, producing a radical anion at m/z 1287. Electron detachment is also prevalent for the singly charged anions, forming unobservable neutral products, and reducing the total ion signal by *ca.* 10% when compared with a spectrum obtained with the laser beam blocked. Like the protonated species, higher photoproduct ion abundance is observed for the lower charge state, specifically 1.6% for singly charged kinetensin anions, compared to 0.2% for the dianions. Unlike the previously published CID spectrum,²⁹ diagnostic sequence ions were not found to be abundant following UV irradiation of the precursor anions.

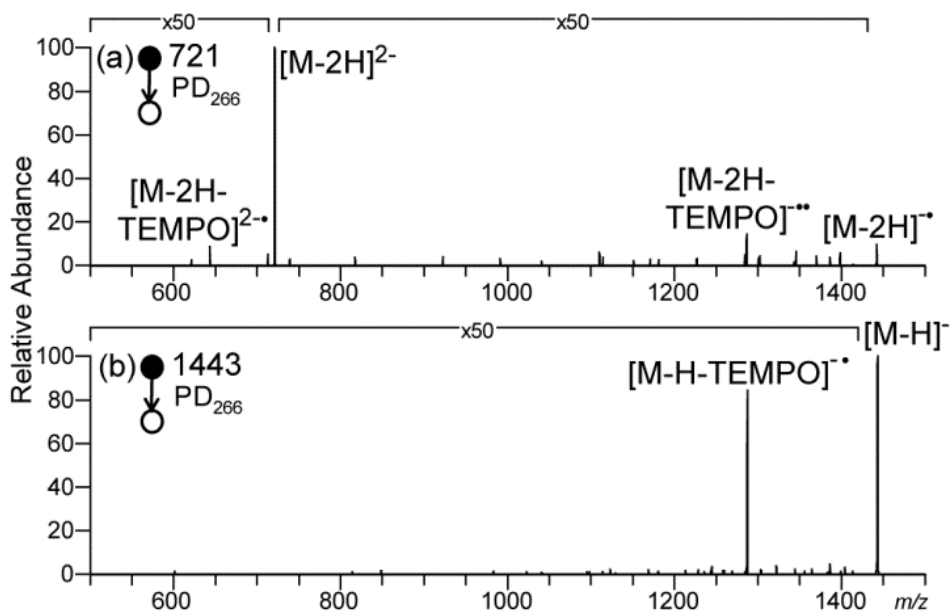


Figure 2: Mass spectra obtained upon isolation and irradiation of deprotonated TEMPO-Bz modified kinetensin (IARRHPYFL) ions, exhibiting ions attributable to bond homolysis and electron detachment; (a) PD₂₆₆ of $[M - 2H]^{2-}$ ions, where the abundance of ions other than m/z 721 and 1442 have been magnified by 50 times; (b) PD₂₆₆ of $[M - H]^{-}$ ions, where the abundance of ions other than m/z 1443 have been magnified by 50 times.

Despite the comparably high selectivity for NO-C bond homolysis observed by both activation methods, the production of peptide radical ions through TEMPO loss (*cf.* Scheme 1) is less prevalent for PD₂₆₆ than for CID. The efficacy of the latter can also be easily modulated, by adjusting the activation energy applied to the trapped ions. The modest yield from PD₂₆₆ irradiation was found to be consistent for all peptides studied, with a small improvement in PD₂₆₆ photoproduct yields for singly charged ions, compared to doubly charged ions. The maximum raw photoproduct ion abundance observed was *ca.* 10.5% relative to the precursor ion, for singly protonated YGGFMRP. By comparison, the radical photoproduct yield of the equivalent $[M + 2H]^{2+}$ ion was only 0.2%, and 2.3% for the $[M - H]^{-}$ ion (see Supporting Information, Figure S3).

Characterisation of radical ions

Despite overall low PD yields, sufficient radical photoproduct ions were produced to enable further interrogation through MS^n experiments in the linear ion trap, and allow comparison of the radical ions initially formed by CID and PD_{266} . Such ions are matched by comparing CID/CID (MS^3) spectra to the equivalent PD_{266}/CID (MS^3) spectra. For example, $[M + 2H]^{2+}$ ions of modified YGGFMRF (m/z 576) are subjected to CID and PD_{266} to form radical ions (m/z 498) *via* loss of TEMPO. Upon subsequent isolation and collisional activation, CID/CID and PD_{266}/CID spectra were acquired. These spectra are compared in Figure 3(a) and 3(b), respectively, and exhibit the same product ions at similar relative abundances. The highest intensity product ion peak is a doubly charged c_6 ion, which can only feasibly be generated by radical-driven processes. Hydrogen atom transfer is proposed to explain the radical mediated backbone cleavage and side chain losses observed in FRIPS, and the relationship to peptide structure.^{26, 55} Independent of charge state, hydrogen atom transfer from the amino acid side chain to the benzylic radical results in a peptide-based radical with a closed-shell *o*-methylbenzamide modification at the *N*-terminus.²⁷ Subsequent β -cleavage of the peptide-based radical yields *a/x*- and *c/z*-type ions. Side chain losses are also observed, with diagnostic mass losses identifying specific amino acid residues, such as the 61 Da loss ($CH_3SCH_2^\bullet$) specific to methionine (Figure 3b). Noticeably, an array of *b*- and *y*-type ions are also observed in both MS^3 spectra. As there are more protons than basic arginine residues, conventional mobile-proton-assisted (rather than radical-driven) backbone dissociation is responsible for the formation of these ions.⁵⁶ Based on the similarities between the two MS^3 spectra, the radical ion species formed by both CID and PD activation methods are identical. Therefore, PD_{266}/CID may be used to obtain the same structural information as CID/CID, albeit with a lower radical ion abundance.

As a further example, the PD₂₆₆/CID spectrum of doubly charged bradykinin is shown in Figure 3(c). Predominantly *a*-type ions are observed, along with *b*-, *c*-, *y*-, and *z*-type ions, as well as radical-driven side chain losses associated with arginine. This MS³ spectrum shares several features with a result obtained by Sun *et al.*, whereby doubly protonated bradykinin radical ions were generated through PD₂₆₆ of a non-covalent complex, and subsequently subjected to CID.⁵⁷ Fragmentation is preferentially observed at aromatic phenylalanine residues, producing *a*₅ and *a*₈ ions. As a consequence of cleavage between phenylalanine and serine, *c*₅ and *z*₄ ions are also observed. The proline effect governs the formation of abundant *y*₈ ions. However, compared to YGGFMRF, *b*-type and *y*-type ions are otherwise suppressed in bradykinin, due to the sequestration of charge on multiple arginine residues. Like bradykinin, the PD₂₆₆/CID spectrum of kinetensin (IARRHPYFL, Figure 3d) is dominated by *a*-type ions, and fragmentation of the side chain of the first amino acid from the *N*-terminus, namely a 29 Da loss (CH₃CH₂[•]) from isoleucine. Other radical-driven side chain losses from tyrosine and arginine are also observed. Comparing with the equivalent CID/CID spectra for bradykinin and kinetensin (Supporting Information, Figure S4 and Figure S5, respectively) confirms that the radical ion species initially produced by CID and PD₂₆₆ are essentially equivalent, and thus provide the same structural information. Importantly, these results confirm that the structure of radical ions produced from TEMPO-Bz derivatives of peptides are identical regardless of the activation method used to generate them. The sensitivity and thus the utility of PD₂₆₆ irradiation is hampered however by the low photoproduct yields; typically less than 5% of the precursor ion abundance.

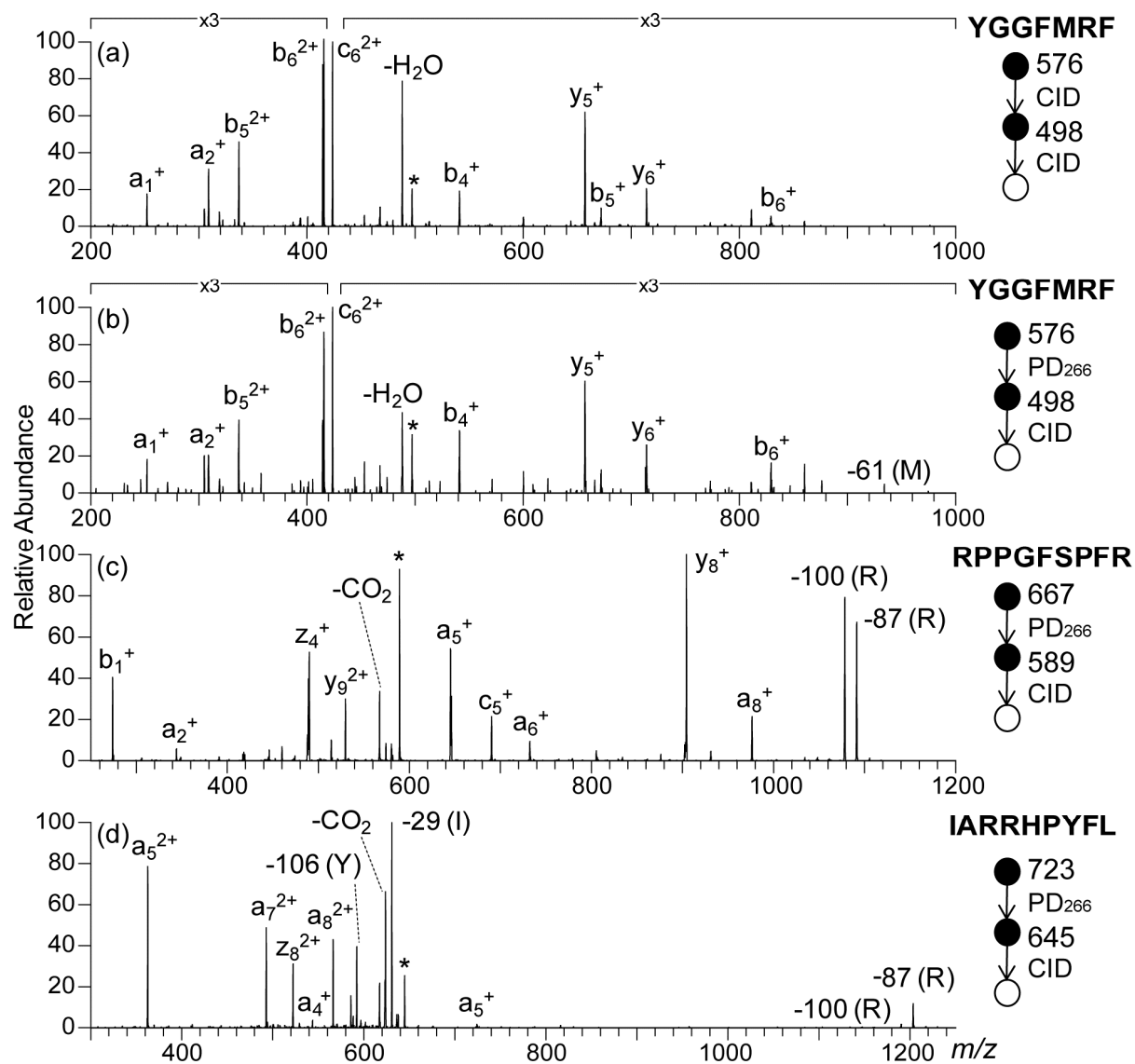


Figure 3: MS³ spectra obtained following CID of $[M + 2H - TEMPO]^{2+}$ radical ions: (a) YGGFMRF, generated by CID; (b) YGGFMRF, generated by PD₂₆₆; (c) bradykinin, generated by PD₂₆₆; (d) kinetensin, generated by PD₂₆₆. Major peptide sequence ions and radical mediated side chain losses are assigned, with the identified amino acid in parentheses. The precursor ion in each spectrum is marked with an asterix (*).

Photodissociation action spectroscopy of derivatised peptides

To investigate the possibility of improving the radical photoproduct yield by varying the incident photon energy, PD action spectra are acquired across a wavelength range of 300 – 220 nm in one nanometre increments. Photofragmentation is not observed when the wavelength is tuned further to the red ($\lambda > 300$ nm), consistent with previous observations of the photolysis of the TEMPO-Bz moiety.⁵⁸ Plotting the power-corrected photodissociation yield of the $[M + 2H - \text{TEMPO}]^{2+\bullet}$ product ion from the $[M + 2H]^{2+}$ ions of both bradykinin and kinetensin against the photon wavelength results in the PD action spectra shown in Figure 4. The maximum photodissociation yield for bradykinin occurs around 227 nm, and for kinetensin around 232 nm. Changes in photodissociation action spectrum profile may be used as indicators for variations in the primary or secondary structure of small peptides.³⁸ Differences in the PD action spectra between kinetensin and bradykinin are qualitatively attributed to the different number and type of aromatic residues (chromophores) in the peptide, and their proximity to the *N*-terminus, where the dissociation occurs. Although it must be noted that the absolute photoproduct yields acquired with different lasers may not be directly comparable, the low photodissociation yield at longer wavelengths correlates with low photoproduct yields observed using the fixed-frequency 266 nm laser (maximum raw photoproduct abundance *ca.* 2% for doubly charged peptide ions). Based on these data, 266 nm does not correspond to the ideal photon energy to efficiently induce dissociation of the NO-C bond in TEMPO-modified peptides with more efficient conversion to the radical ions achieved near 230 – 225 nm (representing an increase in yield of *ca.* 20-50 fold).

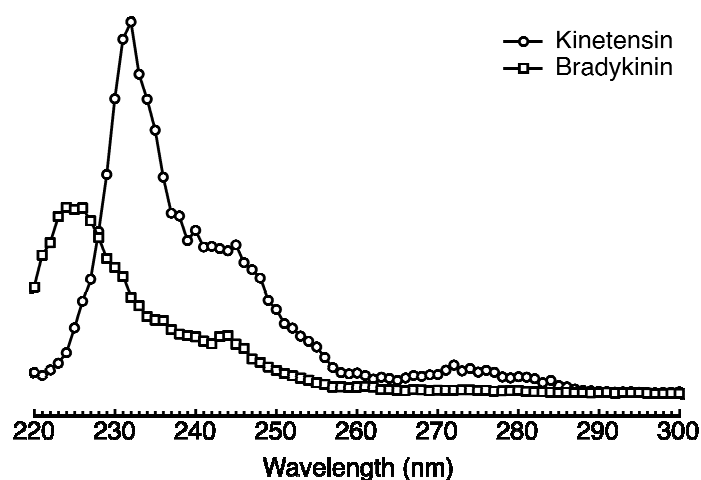


Figure 4: Photodissociation action spectra exhibiting the relative yield of $[M + 2H - \text{TEMPO}]^{2+}$ photoproducts from TEMPO-Bz modified bradykinin and kinetensin $[M + 2H]^{2+}$ ions as a function of wavelength. The PD action spectrum plotting the y_8^+ product ion from bradykinin has a similar profile to that of the $[M + 2H - \text{TEMPO}]^{2+}$ photoproduct ion, both action spectra are compared in Figure S6 in the Supporting Information. Representative photodissociation mass spectra for both TEMPO-Bz modified peptides are also provided as Supporting Information, Figure S7 and Figure S8.

Proteins as large as ubiquitin, modified to contain an iodo-tyrosine residue, produce abundant radical ions upon PD_{266} (at a similar fluence to that employed herein), through homolysis of the aryl carbon-iodine bond on an excited state surface,^{59, 60} which is known to occur on the sub-picosecond timescale following excitation.⁴⁷ By contrast, although the photon energies employed herein ($300 \text{ nm} = 399 \text{ kJ mol}^{-1}$) exceed the NO-C bond dissociation energy in TEMPO-Bz (*ca.* 110 kJ mol^{-1}), the excess energy does not result in the formation of abundant photoproduct ions *via* homolysis. The modest abundance of peptide radical ions by PD may be a result of poor absorption cross-section, or a large population of the ions redistributing their excess energy *via* non-dissociative relaxation pathways (*e.g.*, collisional cooling). Photodissociation of the NO-C bond in the TEMPO-Bz moiety therefore warranted further investigation.

The formation of y_8^+ ions (m/z 904), observed in the CID spectra of both unmodified⁶¹ and TEMPO-Bz modified bradykinin (Figure 1a), also proceeds upon ultraviolet excitation of the latter. Formation of y_8^+ ions as a function of wavelength exhibits a similar profile to that of the TEMPO loss product (see Supporting Information, Figure S6), which suggests that both products are formed by similar processes following photo-excitation. The dissociation to y_n^+ ions is known to be facilitated by vibrational excitation on the electronic ground state surface.⁶² Therefore, TEMPO loss through oxygen-carbon bond dissociation also likely occurs following excitation and internal conversion to a vibrationally-excited electronic ground-state. Previous work has suggested, that the branching ratio between excited state fragmentation and ground state fragmentation is variable, depending on the peptide sequence and conformation, charge state, and charge site.^{63, 64} In some cases, internal conversion is so dominant that excited state-specific fragmentation is completely quenched;⁶² this appears to be the case here. We surmise therefore, that UV photodissociation of the derivatised peptides kinetensin and bradykinin is occurring on their respective ground electronic states. Differences in their photoaction spectra (Figure 4) thus reflect variation in absorption profile, resulting from differences in primary and secondary structure, rather than participation of any particular excited-state dissociation mechanisms.

Photodissociation of model compounds

In order to better understand – and potentially improve – the apparently poor efficiency of NO-C photodissociation in the TEMPO-Bz system, model compounds (**1-3**) were synthesised and subjected to PD₂₆₆ irradiation (Figure 5). Isolation and photodissociation of the $[M - H]^-$ anions formed from 4-carboxy-TEMPO-Bz (**1**) selectively produce radical anions at m/z 199 in modest yield, through cleavage of the NO-C bond and neutral loss of the benzyl radical moiety (Figure 5a). Further interrogation of the m/z 199 ions

by CID resulted in an MS³ (PD₂₆₆/CID) spectrum identical to: (i) the MS³ (CID/CID) spectrum produced by successive CID steps from the same precursor ion (**1**); and (ii) the CID spectrum obtained from the [M – H][–] anion formed by ESI of an authentic sample of 4-carboxy-TEMPO (**1a**) (see Supporting Information, Figure S9). Although much smaller in size than the studied peptides, photodissociation of the NO-C bond in this system indicates that the chromophore present on the TEMPO-Bz linker is also able to initiate homolysis. Therefore, peptides without aromatic residues may also be amenable to photodissociation using this tagging group. With this prototype system, the photoproduct yield is *ca.* 3% relative to the precursor ion and is similar in magnitude to the maximum PD₂₆₆ efficiency observed for the TEMPO-modified peptides. A similarly modest photoproduct yield (*ca.* 4%) is also observed when, for compound (**2**), a cyclohexyl linker is added between TEMPO-Bz and the carboxylate charge carrier (Figure 5b). The TEMPO-Bz moiety does not undergo efficient bond homolysis at 266 nm, despite the stability of the putative distonic nitroxyl radical anion products (**1a**) and (**2a**).⁶⁵ In the third model compound (**3**) an additional aromatic chromophore was installed at the 4-position of the piperidine ring. Compared with (**1**) and (**2**), the benzyl loss photoproduct yield from [M – H][–] anions formed from (**3**) is greatly enhanced, contributing over 50% of the total ion population. In addition to the major photoproduct arising from loss of the benzyl moiety (**3a**), a secondary product ion is also observed at *m/z* 304, corresponding to subsequent loss of a methyl radical. Covalent attachment of an additional aromatic chromophore to the 4-position of the piperidine ring improves the photodissociation yield in the TEMPO-Bz motif more drastically than variation of chromophores on the peptide backbone, potentially through increased absorption cross-section, or by opening up more efficient pathways to NO-C bond homolysis on an excited state surface.^{66, 67}

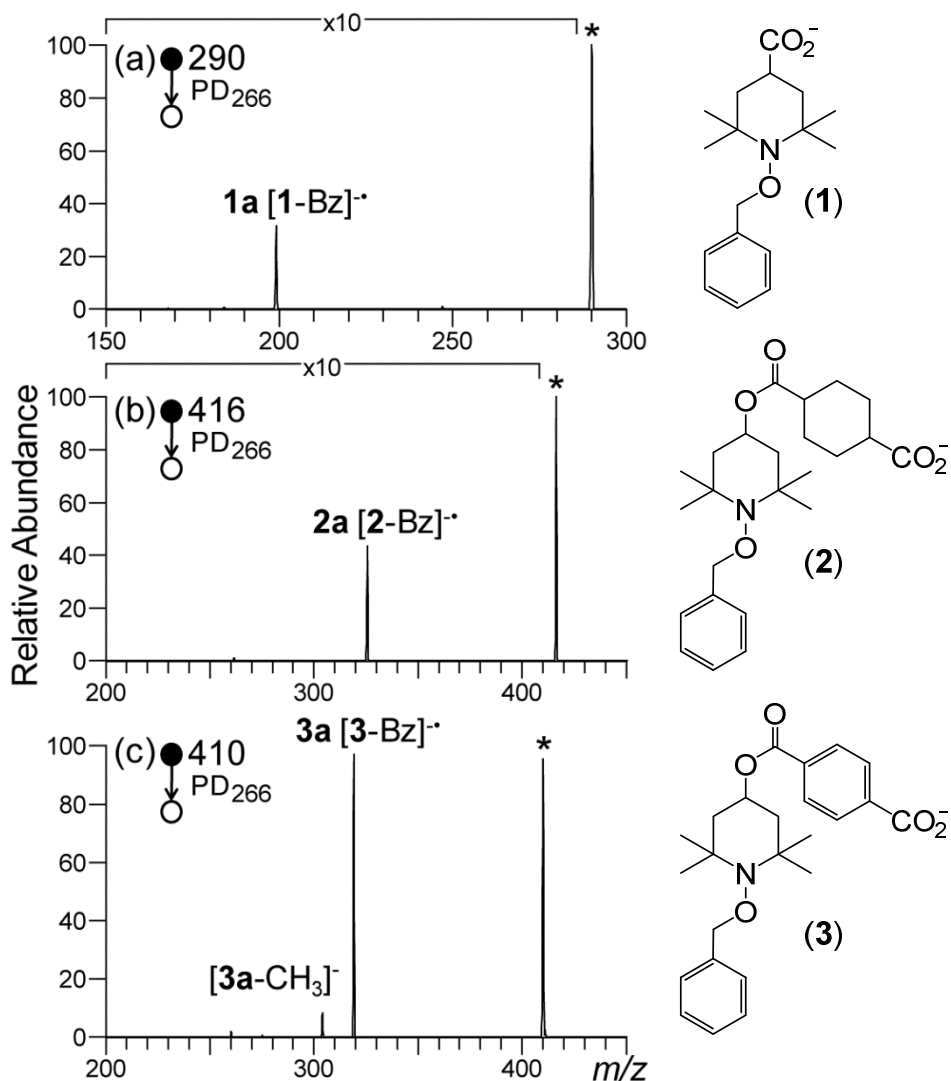


Figure 5: PD₂₆₆ of the [M – H]⁻ anions formed from model TEMPO-Bz compounds **1-3** produce the respective nitroxyl radicals (**1a-3a**): (a) 1-(benzyloxy)-2,2,6,6-tetramethylpiperidine-4-carboxylic acid (**1**); (b) 4-(((1-(benzyloxy)-2,2,6,6-tetramethylpiperidin-4-yl)oxy)carbonyl)cyclohexanecarboxylic acid (**2**); and (c) 4-(((1-(benzyloxy)-2,2,6,6-tetramethylpiperidin-4-yl)oxy)carbonyl)benzoic acid (**3**)

Conclusions

Photodissociation of TEMPO-Bz conjugated peptide ions were carried out in a modified linear ion trap mass spectrometer coupled to two laser systems. Despite modest yields of radical photoproducts, further MSⁿ interrogation confirms the structural identity of the formed radical to be the same as that afforded by CID of the same precursor ion, yielding a similarly informative mass spectrum. Wavelength dependence of the photodissociative radical formation step by action spectroscopy reveals a maximum photoproduct yield around 230 nm, contingent on the charge state and peptide sequence.

The results from photodissociation of model systems suggests that the proximity of additional chromophores improves the efficiency of photodissociation and is consistent with prior observations in both polymers⁶⁸⁻⁷¹ and peptides.^{72, 73} Although the peptides investigated here incorporate aromatic residues, different peptide structures elicit only minor changes in the photodissociation profile. Based on the data in Figure 5, we speculate that an additional chromophore installed within the TEMPO-Bz derivative would increase the radical photoproduct yield when coupled to peptides, due to more efficient energy transfer into the NO-C bond. Extensive dissociation in such systems may even lead to secondary radical-driven fragmentation of the peptide within a single activation step, providing sufficient diagnostic information for peptide sequencing. If realised this scenario could remove the need for subsequent collisional activation and thus avoid the low-mass cut-off inherent in the use of ion traps for CID. These insights will therefore inform future design of more photolabile derivatives that may further enhance the utility of radical-directed dissociation for proteomics applications.

Acknowledgements

D.L.M and C.S.H are supported by Australian Postgraduate Awards. The authors acknowledge the generous financial assistance of the Australian Research Council through the Centre of Excellence for Free Radical Chemistry and Biotechnology (CE0561607) and Discovery grant (DP120102922) schemes with instrumentation supported through the Linkage Infrastructure and Equipment Fund (LE0453832 and LE110100093). H.B.O was supported by the National Research Foundation (NRF) of Korea funded by the Korean government (MOE) (NRF-2012R1A1A2006532).

References

1. S. A. McLuckey and D. E. Goeringer, *J. Mass Spectrom.*, 1997, **32**, 461-474.
2. A. W. Jones and H. J. Cooper, *Analyst*, 2011, **136**, 3419-3429.
3. A. Guthals and N. Bandeira, *Mol. Cell. Proteomics*, 2012, **11**, 550-557.
4. R. A. Zubarev, *Mass Spectrom. Rev.*, 2003, **22**, 57-77.
5. R. A. Zubarev, N. L. Kelleher and F. W. McLafferty, *J. Am. Chem. Soc.*, 1998, **120**, 3265-3266.
6. H. J. Cooper, K. Hakansson and A. G. Marshall, *Mass Spectrom. Rev.*, 2005, **24**, 201-222.
7. H. B. Oh and F. W. McLafferty, *Bull. Korean Chem. Soc.*, 2006, **27**, 389-394.
8. J. J. Coon, J. E. P. Syka, J. Shabanowitz and D. F. Hunt, *BioTechniques*, 2005, **38**, 519-523.
9. J. E. P. Syka, J. J. Coon, M. J. Schroeder, J. Shabanowitz and D. F. Hunt, *Proc. Natl. Acad. Sci. USA*, 2004, **101**, 9528-9533.
10. R. A. Zubarev, D. M. Horn, E. K. Fridriksson, N. L. Kelleher, N. A. Kruger, M. A. Lewis, B. K. Carpenter and F. W. McLafferty, *Anal. Chem.*, 2000, **72**, 563-573.
11. H. Lioe and R. A. J. O'Hair, *Anal. Bioanal. Chem.*, 2007, **389**, 1429-1437.
12. T. Ly, S. Yin, J. A. Loo and R. R. Julian, *Rapid Commun. Mass Spectrom.*, 2009, **23**, 2099-2101.
13. A. Kalli, G. Grigorean and K. Hakansson, *J. Am. Soc. Mass. Spectrom.*, 2011, **22**, 2209-2221.
14. I. K. Chu, C. F. Rodriguez, T. C. Lau, A. C. Hopkinson and K. W. M. Siu, *J. Phys. Chem. B*, 2000, **104**, 3393-3397.
15. J. Laskin, Z. Yang and I. K. Chu, *J. Am. Chem. Soc.*, 2008, **130**, 3218-3230.
16. A. C. Hopkinson, *Mass Spectrom. Rev.*, 2009, **28**, 655-671.
17. S. Wee, R. A. J. O'Hair and W. D. McFadyen, *Int. J. Mass Spectrom.*, 2004, **234**, 101-122.
18. C. K. Barlow, D. Moran, L. Radom, W. D. McFadyen and R. A. J. O'Hair, *J. Phys. Chem. A*, 2006, **110**, 8304-8315.
19. R. P. W. Kong, Q. Quan, Q. Hao, C. K. Lai, C. K. Siu and I. K. Chu, *J. Am. Soc. Mass. Spectrom.*, 2012, **23**, 2094-2101.
20. S. Osburn, R. A. J. O'Hair and V. Ryzhov, *Int. J. Mass Spectrom.*, 2012, **316**, 133-139.
21. V. Ryzhov, A. K. Y. Lam and R. A. J. O'Hair, *J. Am. Soc. Mass. Spectrom.*, 2009, **20**, 985-995.
22. E. R. Knudsen and R. R. Julian, *Int. J. Mass Spectrom.*, 2010, **294**, 83-87.
23. G. Hao and S. S. Gross, *J. Am. Soc. Mass. Spectrom.*, 2006, **17**, 1725-1730.
24. A. W. Jones, P. J. Winn and H. J. Cooper, *J. Am. Soc. Mass. Spectrom.*, 2012, **23**, 2063-2074.
25. A. Chacon, D. S. Masterson, H. Y. Yin, D. C. Liebler and N. A. Porter, *Biorg. Med. Chem.*, 2006, **14**, 6213-6222.
26. R. Hodyss, H. A. Cox and J. L. Beauchamp, *J. Am. Chem. Soc.*, 2005, **127**, 12436-12437.
27. M. Lee, M. Kang, B. Moon and H. B. Oh, *Analyst*, 2009, **134**, 1706-1712.
28. M. Lee, Y. Lee, M. Kang, H. Park, Y. Seong, B. J. Sung, B. Moon and H. B. Oh, *J. Mass Spectrom.*, 2011, **46**, 830-839.
29. J. Lee, H. Park, H. Kwon, G. Kwon, A. Jeon, H. I. Kim, B. J. Sung, B. Moon and H. B. Oh, *Anal. Chem.*, 2013, **85**, 7044-7051.
30. T. R. Rizzo, J. A. Stearns and O. V. Boyarkin, *Int. Rev. Phys. Chem.*, 2009, **28**, 481-515.

31. J. J. Wilson and J. S. Brodbelt, *Anal. Chem.*, 2007, **79**, 7883-7892.
32. J. P. Reilly, *Mass Spectrom. Rev.*, 2009, **28**, 425-447.
33. D. J. Nesbitt and R. W. Field, *J. Phys. Chem.*, 1996, **100**, 12735-12756.
34. R. Antoine, L. Joly, T. Tabarin, M. Broyer, P. Dugourd and J. Lemoine, *Rapid Commun. Mass Spectrom.*, 2007, **21**, 265-268.
35. T. Ly and R. R. Julian, *J. Am. Chem. Soc.*, 2008, **130**, 351-358.
36. T. Ly and R. R. Julian, *J. Am. Soc. Mass. Spectrom.*, 2009, **20**, 1148-1158.
37. T. Ly and R. R. Julian, *J. Am. Chem. Soc.*, 2010, **132**, 8602-8609.
38. B. B. Kirk, A. J. Trevitt, S. J. Blanksby, Y. Tao, B. N. Moore and R. R. Julian, *J. Phys. Chem. A*, 2013, **117**, 1228-1232.
39. K. K. Thoen, J. Pérez, J. J. Ferra Jr and H. I. Kenttämä, *J. Am. Soc. Mass. Spectrom.*, 1998, **9**, 1135-1140.
40. M. B. Prendergast, P. A. Cooper, B. B. Kirk, G. d. Silva, S. J. Blanksby and A. J. Trevitt, *Phys. Chem. Chem. Phys.*, 2013, **15**, 20577-20584.
41. T. Ly, X. Zhang, Q. Sun, B. Moore, Y. Tao and R. R. Julian, *Chem. Commun.*, 2011, **47**, 2835-2837.
42. Y.-H. Yang, K. Lee, K.-S. Jang, Y.-G. Kim, S.-H. Park, C.-S. Lee and B.-G. Kim, *Anal. Biochem.*, 2009, **387**, 133-135.
43. B. Moore, Q. Sun, J. C. Hsu, A. H. Lee, G. C. Yoo, T. Ly and R. R. Julian, *J. Am. Soc. Mass. Spectrom.*, 2012, **23**, 460-468.
44. J. K. Diedrich and R. R. Julian, *Anal. Chem.*, 2010, **82**, 4006-4014.
45. K.-U. Schoening, W. Fischer, S. Hauck, A. Dichtl and M. Kuepfert, *J. Org. Chem.*, 2008, **74**, 1567-1573.
46. T. Ly, B. B. Kirk, P. I. Hettiarachchi, B. L. J. Poad, A. J. Trevitt, G. da Silva and S. J. Blanksby, *Phys. Chem. Chem. Phys.*, 2011, **13**, 16314-16323.
47. C. S. Hansen, B. B. Kirk, S. J. Blanksby, R. A. J. O'Hair and A. J. Trevitt, *J. Am. Soc. Mass. Spectrom.*, 2013, **24**, 932-940.
48. D. G. Harman and S. J. Blanksby, *Org. Biomol. Chem.*, 2007, **5**, 3495-3503.
49. J. L. Hodgson, L. B. Roskop, M. S. Gordon, C. Y. Lin and M. L. Coote, *J. Phys. Chem. A*, 2010, **114**, 10458-10466.
50. V. Katta, S. K. Chowdhury and B. T. Chait, *Anal. Chem.*, 1991, **63**, 174-178.
51. J. Seidler, N. Zinn, M. E. Boehm and W. D. Lehmann, *Proteomics*, 2010, **10**, 634-649.
52. T. A. Lowe, M. R. L. Paine, D. L. Marshall, L. A. Hick, J. A. Boge, P. J. Barker and S. J. Blanksby, *J. Mass Spectrom.*, 2010, **45**, 486-495.
53. A. Jeon, J. H. Lee, H. S. Kwon, H. S. Park, B. J. Moon and H. B. Oh, *Mass Spectrom. Lett.*, 2013, **4**, 71-74.
54. J. Laskin, Z. Yang, C. Lam and I. K. Chu, *Anal. Chem.*, 2007, **79**, 6607-6614.
55. H. Yin, A. Chacon, N. A. Porter, H. Y. Yin and D. S. Masterson, *J. Am. Soc. Mass. Spectrom.*, 2007, **18**, 807-816.
56. V. H. Wysocki, G. Tsapralis, L. L. Smith and L. A. Breci, *J. Mass Spectrom.*, 2000, **35**, 1399-1406.
57. Q. Sun, H. Nelson, T. Ly, B. M. Stoltz and R. R. Julian, *J. Proteome Res.*, 2009, **8**, 958-966.
58. J. C. Scaiano, T. J. Connolly, N. Mohtat and C. N. Pliva, *Can. J. Chem.*, 1997, **75**, 92-97.
59. Q. Sun, S. Yin, J. A. Loo and R. R. Julian, *Anal. Chem.*, 2010, **82**, 3826-3833.
60. T. Ly and R. R. Julian, *Angew. Chem. Int. Ed.*, 2009, **48**, 7130-7137.
61. B. B. Schneider, D. J. Douglas and D. D. Y. Chen, *J. Am. Soc. Mass. Spectrom.*, 2001, **12**, 772-779.
62. S. Park, W.-K. Ahn, S. Lee, S. Y. Han, B. K. Rhee and H. B. Oh, *Rapid Commun. Mass Spectrom.*, 2009, **23**, 3609-3620.
63. R. Antoine, M. Broyer, J. Chamot-Rooke, C. Dedonder, C. Desfrancois, P. Dugourd, G. Gregoire, C. Jouvét, D. Onidas, P. Poulain, T. Tabarin and G. van der Rest, *Rapid Commun. Mass Spectrom.*, 2006, **20**, 1648-1652.

64. L. Joly, R. Antoine, M. Broyer, P. Dugourd and J. Lemoine, *J. Mass Spectrom.*, 2007, **42**, 818-824.
65. G. Gryn'ova, D. L. Marshall, S. J. Blanksby and M. L. Coote, *Nature Chem.*, 2013, **5**, 474-481.
66. S. Hu, J. H. Malpert, X. Yang and D. C. Neckers, *Polymer*, 2000, **41**, 445-452.
67. A. Goto, J. C. Scaiano and L. Maretti, *Photochem. Photobiol. Sci.*, 2007, **6**, 833-835.
68. Y. Guillaneuf, D. Bertin, D. Gigmes, D.-L. Versace, J. Lalevée and J.-P. Fouassier, *Macromolecules*, 2010, **43**, 2204-2212.
69. Y. Guillaneuf, D.-L. Versace, D. Bertin, J. Lalevée, D. Gigmes and J.-P. Fouassier, *Macromol. Rapid Commun.*, 2010, **31**, 1909-1913.
70. J. Nicolas, Y. Guillaneuf, C. Lefay, D. Bertin, D. Gigmes and B. Charleux, *Prog. Polym. Sci.*, 2013, **38**, 63-235.
71. D. L. Versace, Y. Guillaneuf, D. Bertin, J. P. Fouassier, J. Lalevee and D. Gigmes, *Org. Biomol. Chem.*, 2011, **9**, 2892-2898.
72. J. Y. Oh, J. H. Moon, Y. H. Lee, S. W. Hyung, S. W. Lee and M. S. Kim, *Rapid Commun. Mass Spectrom.*, 2005, **19**, 1283-1288.
73. L. Vasicek and J. S. Brodbelt, *Anal. Chem.*, 2010, **82**, 9441-9446.